Science in China Series B: Chemistry

www.scichina.com
chem.scichina.com
www.springerlink.com

Synthesis, crystal structures and electrochemical properties of two new metal-centered ferrocene complexes

WANG XuChun[1,2], WU JieYing[1†], ZHOU HongPing[1†], TIAN YuPeng[1,3], LI Lin[1], YANG JiaXiang[1], JIN BaoKang[1] & ZHANG ShengYi[1]

[1] Department of Chemistry, Anhui Province Key Laboratory of Function Inorganic Material Chemistry, Anhui University, Hefei 230039, China;
[2] Department of Chemistry, Anhui Science and Technology University, Fengyang 233100, China;
[3] State Key Laboratory of Crystal Materials, Institute of Crystal Materials of Shandong University, Jinan 250100, China

Two new metal-centered ferrocene complexes $Ni(SCN)_2(L)_4$ (1) and $Cu(OAc)_2(L)_2$ (2) (L = 1-[1-ferrocenylmethyl]imidazole) have been synthesized and characterized by elemental analysis, single crystal X-ray diffraction analysis, spectroscopic and cyclic voltammetric measurements. The geometry of Ni(II) in 1 is octahedral, with four ligands in the equatorial plan and two thiocyanate anions at the axial site, while that of Cu(II) in 2 is a distorted octahedron formed by two chealted OAc^- and two ligands. Single crystal X-ray diffraction studies reveal that there is partial electron delocalization from ferrocene to imidazole in the two complexes. Electrochemical measurements exhibit that complexes 1 and 2 undergo similar reversible one electron redox processes, suggesting that the ferrocene moieties are equivalent and there are no interactions among them.

ferrocene, imidazole, complex, crystal structure, electrochemistry

1 Introduction

The design and syntheses of functional complexes, constructed from multi-ferrocene ligands and transition metals, have attracted much interest because of their potential applications as electron reservoirs[1,2], sensitive electrochemical probes[3,4], ionic liquids[5−7], nonlinear optical materials[8,9], catalysts[10] and building blocks for molecular electronic devices[11−15]. The redox between the ferrocene (Fe(II)) and ferrocenium (Fe(III)), with fast and reversible electron transfer, is one of the important properties of ferrocene derivatives. Recently, more attentions have been focused on the possibility that inorganic and organic redox-active centers could be combined in a single molecular entity[16]. However, it is difficult to model the structural and functional aspects of multiferrocene complexes, in spite of their advantages of tunable composition, geometry and intramolecular electron transfer processes[17−19].

In addition, the organic-inorganic hybridized coordination complexes containing imidazole derivatives, which were designed based on topologies, have been frequently reported[20−24]. In our previous studies, we have successfully designed and synthesized a functional imidazole ligand, and obtained a series of organic-inorganic hybridized supramolecular polymers[25,26], which are different from other reported imidazole-containing coordination polymers[27,28]. Although the functionalized ligand, 1-[1-ferrocenylmethyl]imidazole, has been re-

Received October 6, 2008; accepted November 29, 2008
doi: 10.1007/s11426-009-0091-2
†Corresponding author (email: jywu1957@163.com; zhpzhp@263.net; wxchun2004@163.com)
Supported by the National Natural Science Foundation of China (Grant Nos. 50532030, 50703001, and 20771001), the Team for Scientific Innovation Foundation of Anhui Province (2006KJ007TD), Doctoral Program Foundation of the Ministry of Education of China (20050357001) and Education Committee of Anhui Province (KJ2009B167Z)

ported[29], little studies on synthesis of ferrocenyl imidazole complexes have been involved. Therefore, we have carried out research on the rational design and synthesis of these complexes which incorporate ferrocene, imidazole and inorganic salt into one molecule by the self-assembling procedure. The combination of inorganic and functional organic moieties leads to both unique structural architectures and improved properties. This article studies the synthesis, X-ray characterizations and electrochemical properties of two new ferrocenyl imidazole complexes $Ni(SCN)_2(L)_4$ (**1**) and $Cu(OAc)_2(L)_2$ (**2**).

2 Experimental

All used chemicals were of analytical grade. The solvents were purified as conventional methods before use. Ferrocene carboxaldehyde and Ferrocenecarbinol were prepared in an analogous way to that of literature[30,31]. We prepared the electron-active ligand, 1-[1-ferrocenylmethyl]imidazole (**L**), by using modified procedure[27]. Elemental analyses (C, H, N) were performed using a Perkin Elmer 240B elemental analyzer. IR spectra were obtained on a Nicolet Nexus-870 spectrometer with samples prepared as KBr pellets. ^{1}H NMR spectra were obtained on a Bruker Advance/DMX 500 NMR spectrometer in $CDCl_3$ solution. Electronic spectra were recorded on a UV-265 spectrophotometer. The cyclic voltammograms (CV) were obtained on an EG&G PAR 283 potentiostat at room temperature, using CH_2Cl_2 as solvent and 0.1 mol·L^{-1} Bu_4NClO_4 as supporting electrolyte. The potentials were referred to an Ag-AgCl electrode. A platinum-wire auxiliary electrode was used in conjunction with a platinum-disk-working. The cyclic voltammograms of freshly prepared (1 mmol·L^{-1}) solution of the compounds in solution were recorded at 0.05 V·s^{-1} in the range of 0–1400 mV.

2.1 Synthesis of 1-[1-ferrocenylmethyl] imidazole (L)

The ligand was prepared by modified procedure: Ferrocenecarbinol (1.08 g, 5 mmol) and imidazole (0.480 g, 7 mmol) were dissolved in 5 mL of acetic acid and stirred at 60℃ for 12 h, and then volatiles were removed under reduced pressure. $NaHCO_3$ solution and CH_2Cl_2 were added, and the layers were separated. The organic layer was collected, dried over $MgSO_4$ and evaporated. The residue was purified by flash chromatography with light petroleum/ethyl acetate (2∶1) as eluent, and gave the compound L as yellow-brown solid. Yield: 0.96 g (72%), m.p. 66－67℃. Brown needle-shaped crystals of **L** suitable for X-ray crystallographic analysis were obtained by slow evaporation of cyclohexane into a CH_2Cl_2 solution containing the corresponding compound at room temperature after a week. MS: (EI, 70 eV): *m*/*z*, 266 [M], 199 ($FcCH_2$). Anal for $C_{14}H_{14}FeN_2$: C, 63.19; H, 5.30; N, 10.53%. Found: C, 63.02; H, 5.46; N, 10.29%. IR (KBr, cm^{-1}): 3401 (m), 3100 (m), 1666 (m), 1587 (m), 1506 (s), 1434 (m), 1269 (s), 1216 (s), 1103 (s), 1028 (s), 989 (m), 815 (s), 741 (s), 658 (m). ^{1}H NMR (500 MHz, $CDCl_3$) δ: 7.52 (s, 1 H), 7.26 (d, 1 H, J = 7.1 Hz), 6.35 (d, 1 H, J = 7.1 Hz), 4.87 (s, 2 H), 4.19 (m, 3 H), 4.17 (s, 5 H), 4.16 (m, 1 H).

2.2 Synthesis of $Ni(SCN)_2L_4$ (1)

A clear methanol solution (15 mL) of $Ni(SCN)_2$ (0.0174 g, 0.1 mmol) was carefully layered onto a solution of L (0.106 g, 0.4 mmol) in chloroform (15 mL). Red needle-shaped crystals of **1** suitable for X-ray crystallographic analysis were obtained by slow interlayer diffusion. Yield: 70%; m.p. 149－151℃. Anal. Calc. for $C_{58}H_{56}Fe_4N_{10}NiS_2$: C, 56.21; H, 4.55; N, 11.30%. Found: C, 56.06; H, 4.58; N, 11.15%. IR (KBr, cm^{-1}): 3402 (m), 3100 (m), 2122 (s), 1752 (m), 1673 (s), 1379 (s), 1303 (m), 1102 (s), 1017 (s), 820 (s), 751 (s), 665 (m).

2.3 Synthesis of $Cu(OAc)_2(L)_2$ (2)

The preparation of $Cu(OAc)_2(L)_2$ was analogous to the procedure of **1**. A clear methanol solution (15 mL) of $Cu(OAc)_2·H_2O$ (0.0197 g, 0.1 mmol) was carefully layered onto a solution of **L** (0.0532 g, 0.2 mmol) in chloroform (15 mL). Orange needle-shaped crystals suitable for X-ray crystallographic analysis were obtained by slow interlayer diffusion. Yield: 65%; m.p. 159－161℃. Anal. Calc. for $C_{32}H_{34}CuFe_2N_4O_4$: C, 53.84; H, 4.80; N, 7.85%. Found: C, 53.68; H, 4.72; N, 7.91%. IR (KBr, cm^{-1}): 3447 (m), 2963 (m), 1620 (s), 1517 (m), 1425 (m), 1262 (s), 1100 (s), 1022 (s), 819 (m), 806 (s), 722 (m), 677 (m).

2.4 X-ray crystal structure determinations

Single-crystal X-ray diffraction measurements were performed on a Bruker SMART CCD detector using graphite monochromated Mo$K\alpha$ radiation (λ = 0.71073 Å) at 298 K. The data were collected on a SMART diffractometer using the phi and omega technique. The structures have been solved by SHELXS-97 and refined using SHELXL-97 program package[32]. All non-hydro-

Table 1 Crystallographic data and structure refinement summary for **1** and **2**

Compound	1	2
Formula	$C_{58}H_{56}Fe_4N_{10}NiS_2$	$C_{32}H_{34}CuFe_2N_4O_4$
CCDC No.	276330	609285
Formula weight	1239.36	713.87
T(K)	298(2)	298(2)
Crystal system	monoclinic	monoclinic
Space group	$P2_1/n$	$C2/c$
a (Å)	18.088(6)	20.972(5)
b (Å)	9.069(3)	7.720(1)
c (Å)	18.711(6)	21.536(5)
β (°)	116.009(4)	116.862(3)
V (Å^3)	2758.6(14)	3110.5(12)
Z	2	4
D_{calc} (g·cm^{-3})	1.492	1.524
θ range (°)	1.31－25.10	2.12－25.01
Total No. of data	14001	7819
No. of unique data	4887	2736
No. of para refined	341	196
R_1	0.0632	0.0403
wR_2	0.1491	0.0930
Gof	1.022	1.047

$\alpha R_1=\Sigma \| Fo- \| Fc \| /\Sigma | Fo |$; $wR_2{}^b=[\Sigma(w(Fo^2-Fc^2)^2)/\Sigma(w(Fo^2)^2)]^{1/2/K}$.

Table 2 Selected bond lengths (Å) and bond angles (°) of **1** and **2**

1			
Ni(1)－N(1)	2.087(5)	S(1)－C(1)	1.630(6)
Ni(1)－N(2)	2.090(5)	N(1)－C(1)	1.157(7)
Ni(1)－N(4)	2.115(4)	N(2)－C(2)	1.301(7)
N(2)－C(4)	1.364(8)	N(3)－C(2)	1.340(8)
N(3)－C(3)	1.359(8)	N(3)－C(5)	1.463(8)
C(3)－C(4)	1.345(9)	C(5)－C(6)	1.515(11)
C(6)－C(7)	1.418(12)	C(8)－C(9)	1.407(12)
C(9)－C(10)	1.428(12)	N(1)－Ni(1)－N(2)	90.6(2)
N(2)－Ni(1)－N(4)	88.4 (1)	N(1)－Ni(1)－N(4)	89.9(1)
N(3)－C(5)－C(6)	114.5(6)	N(5)－C(19)－C(20)	112.9(5)
2			
Cu(1)－N(1)	1.994(3)	Cu(1)－O(1)	2.151(4)
Cu(1)－O(2)	2.402(5)	N(1)－C(1)	1.313(4)
N(1)－C(3)	1.369(5)	N(2)－C(1)	1.334(4)
N(2)－C(2)	1.357(5)	N(2)－C(4)	1.481(4)
O(1)－C(15)	1.222(5)	O(2)－C(15)	1.220(5)
C(15)－C(16)	1.466(6)	C(2)－C(3)	1.344(5)
C(4)－C(5)	1.491(5)	C(5)－C(6)	1.413(5)
C(8)－C(9)	1.420(6)	N(1)－Cu(1)－O(1)	90.23(2)
N(1)－Cu(1)－O(2)	89.21(2)	O(1)－Cu(1)－O(2)	55.06(3)
N(2)－C(4)－C(5)	111.5(3)	O(2)－C(15)－O(1)	120.2(5)
O(2)－C(15)－C(16)	119.0(5)	O(1)－C(15)－C(16)	120.8(5)
C(6)－C(5)－C(4)	126.3(4)		

gen atoms were refined anisotropically. All hydrogen atoms were generated in idealized positions. Details of the X-ray crystal data collections and unit-cell parameters are summarized in Table 1, and selected bond distances and angles are listed in Table 2.

3 Results and discussion

3.1 General characterization

Complexes **1** and **2** can all dissolve in common solvents, such as acetone, acetonitrile, methanol, methylene chloride, DMF, and DMSO. The solubility of **2** is superior to that of analogous polymers[33]. The IR spectra of complexes **1** and **2** were listed in synthetic section. The spectra bands at 1265－1601 cm^{-1} can be assigned to the vibration of the benzene and imidazole. The peaks at 1102, 1017, 820 cm^{-1} for **1**, and 1100, 1022, 819 cm^{-1} for **2**, respectively, are assigned to ν_{as} of ferrocene group. The absorption peak at 2122 cm^{-1} is the C－N stretching vibration of SCN^- in complex **1**. For complex **2**, the strong absorption bands at 1620 and 1425 cm^{-1} are assigned to $\nu_{as}(COO^-)$ and $\nu_s(COO^-)$ vibrations, respectively, and the value of $\Delta\nu$ = 195 cm^{-1} (< 200 cm^{-1}) implies chelating mode of OAc^- in accordance with the results of X-ray analysis. The UV-vis peaks (λ_{max}) of the **L**, **1** and **2** (1.0×10^{-5} mol·L^{-1} in DMF) appear at 271 nm ($\varepsilon = 5.2 \times 10^4$), 311 nm ($\varepsilon = 9.5 \times 10^4$) and 315 nm ($\varepsilon = 9.1 \times 10^4$), respectively. The maximum absorption bands can be assigned to the π-π* transition. The complexes **1** and **2** showed red shifts (40 and 44 nm respectively) in absorption, compared with the ligand, which due to the metal ions decreased the charge density and partial electron delocalization in both complexes.

3.2 Crystal structures

(i) Structure of the nickel complex $Ni(SCN)_2L_4$ (**1**). The ORTEP drawings of the structure of complex **1** with the atomic numbering scheme are shown in Figure 1. Selected bond lengths and angles for **1** are included in Table 2. The geometry of the nickel ion in **1** is an octahedral, and four ligands and two thiocyanate anions are coordinated to the equatorial and axial positions, respectively, with six Ni－N bonds from 2.087(5) to 2.115(4) Å. These bond lengths and angles around the Ni atom show normal values[34]. The geometrical characteristics of both imidazole and ferrocenyl moieties in complex **1** and its ligand **L** are very similar. In two cases the Cp-rings of ferrocenyl group are in the eclipsed confor-

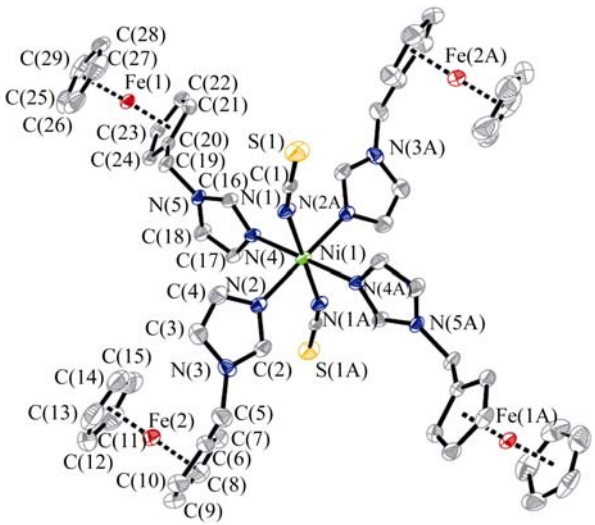

Figure 1 ORTEP drawing of **1**. The thermal ellipsoids are drawn at 30% probability level. All hydrogens were omitted for clarity. Symmetry operations applied to generated equivalent atoms: (symmetry code A) 2–*x*, 1–*y*, –*z*.

mations (Table 2). The dihedral angles between the imidazole planes and Cp-rings are equal to 114.5°, 112.9° for complex **1**, and 110.0° for ligand **L**[29], respectively. The bond length of N(3)—C(5) is 1.463(8) Å, which is shorter than a normal C—C single bond distance (1.53 Å) and longer than a normal double bond distance (1.32 Å), which is also is shorter than its correspondence bond distance N(1)—C(6) (1.474(4) Å) in ligand **L**. The coordination effects, such as σ and $\pi_{M\rightarrow L}$ back bonding in the coordination bond with the centre Ni(II) ion, may lead to slight changes in the bond angles C(Fc)—C(bridge)—N(imidazole) and bond length C(bridge)—N(imidazole)[35,36].

In the crystal structure, the molecules are stacked through hydrogen bond interactions. One interaction is C(Fc)—H···S(SCN) hydrogen bond, with the distance of H···S is 2.851(2) Å and bond angle ∠C—H···S is 148.8(1)° (Table 3). Another is defined by C(imidazole)—H···S(SCN) hydrogen bond, with the distance of H···S is 2.945(2) Å, and bond angle ∠C—H···S is 150.6(1)°. Taking the van der Waals radii of H and S to be 1.20 and 2.05 Å, respectively, any H···S contact of less than 3.25 Å and C—H···S angle greater than 130° can therefore be considered as being significant[37]. The C—H···S hydrogen bond is very important in supramolecular self-assembly[38,39].

Table 3 Intermolecular interaction distances (Å) of complex **1**

D—H···A	Symmetry	D—H	H···A	D···A	D—H···A
C^a—H(21)···S^b	1.5-*x*,-1/2+*y*, 1/2-*z*;-1/2+*x*, 1.5-*y*,1/2+*z*	0.929 (2) Å	2.851 (2) Å	3.677 (2) Å	148.8(1)°
C^c—H(2)··· S^b	1.5-*x*,-1/2+*y*, 1/2-*z*;1.5-*x*, 1/2+*y*,1/2-*z*	0.930 (2) Å	2.945 (2) Å	3.781 (2) Å	150.6(1)°

C^a = C(Fc), S^b = S(SCN), C^c = C(imidazole).

(ii) Structure of the copper complex $Cu(OAc)_2(L)_2$ (**2**). An ORTEP view of **2** with the atomic numbering scheme is shown in Figure 2. The coordination environment around the copper atom of **2** is a strongly distorted octahedron with six bonds formed by two nitrogen atoms from two ligands (Cu—N: 1.994(3) Å), and four oxygen atoms from two chelating acetate. The Cu—O bond distance (2.402(5) Å) of the axial coordination sites is markedly longer than that (Cu—O: 2.151(4) Å) of the equatorial ones. The difference in the Cu—O distances (0.25 Å) is similar to those observed in other six-coordinated Cu(Ⅱ) complexes[40]. The average dihedral angle between the chelating ring (O1, C15, O2, Cu) and the imidazole rings is 85.59°. The two ligands have opposite orientations in complex **2**, and the dihedral angle between Cp ring and imidazole ring in the same ligand is 111.5°, which slightly increased compared with those of complex **1** and the free ligand **L**. In addition, like complex **1**, the bond lengths of N(2)—C(4) and C(4)—C(5) are 1.481(4) and 1.491(5) Å, respectively, which is also shorter than a normal C—C single bond distance (1.53 Å) and longer than a normal double bond distance (1.32 Å). And the coordinated bond Cu(1)—N(1) (1.994(3) Å) is shorter than the Cu—N(3) and Cu—N(5) (2.035(3) and 2.036(3) Å) of

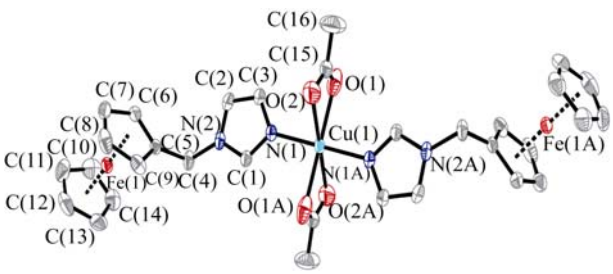

Figure 2 ORTEP drawing of **2**. The thermal ellipsoids are drawn at the 30% probability level. All hydrogens were omitted for clarity. Symmetry operations applied to generated equivalent atoms: (symmetry code A) 0.5–*x*, 0.5–*y*, –*z*.

$(L1)_3Cu(NO_3)_2$ (L1 = 5-ferrocenylpyrimidine)[41]. These structural features in complexes **1** and **2** indicate that there is partial delocalization of electrons from the ferrocene to imidazole[42].

3.3 Electrochemical properties

Electrochemical data for complexes **1** and **2** (1 mmol·L^{-1}), as well as those for the free **L** (1 mmol·L^{-1}) in CH_2Cl_2 solution containing 0.1 mol·L^{-1} Bu_4NClO_4 (TBAP) as supporting electrolyte at an Ag/AgCl electrode in the range of 0—1400 mV, are shown in Table 4 and Figure 3. The half-wave potentials ($E_{1/2}$) of the redox processes and the separation between consecutive waves (ΔE) vary depending on the nature of the complexes and their geometric structures. The internal standard, ferrocene, undergoes a reversible one-electron oxidation as expected (E_{pa} = 0.470 V, E_{pc} = 0.362 V, scanning rate 50 mV·s^{-1}). The ligand undergoes a reversible one-electron oxidation (E_{pa} = 0.536 V, E_{pc} = 0.461 V, scanning rates, 50 mV·s^{-1}). Due to the partial charge transfer from ferrocene to imidazole, the redox potentials of the ligand slightly shift to positive potential. Complexes **1** and **2** exhibit similar reversible one electron redox processes, and shift to positive potential compared with ferrocene. The large peak-to-peak separations ($\Delta E_p = E_{pa} - E_{pc}$) of 111 mV for **1** and 118 mV for **2**, might suggest that these peaks were not simple reversible one-electron reactions, because the small ΔE_p value (36 mV) between two voltammetric waved always led to the two waves coupled each other and only one broad voltammetric wave appeared in the cyclic voltammetry measurements[38]. In this case, the only one broad voltammetric wave in the each complex indicates that the ferrocene moieties are identical and there is no interaction between them.

The half-wave potential value ($E_{1/2}$) of complex **1** is observed at 0.478 V, which is more negative than that of the ligand ($E_{1/2}$ = 0.500 V), indicating that the complex tend to be oxidized even more than the ligand. But the value ($E_{1/2}$ = 0.667 V) of complex **2** is higher than that of the ligand, indicating that the oxidation and reduction of **2** are more difficult than those of ligand. It is postulated that the $E_{1/2}$ (ΔE_p) depends on a number of factors such as bond making and breaking, changes in coordination number, severe changes in coordination geometry, and electronic delocalization in oxidation states[43]. First, crystal structure analysis indicates that the metal-iron and iron-iron distances as well as the bond distances of the ferrocene moieties are almost equivalent for complexes **1** and **2**, the metal-iron and iron-iron distance are not the important factors influence the redox potentials of these kind of multi-ferrocene complexes. The difference in electrochemistry of complexes **1** and **2** may be described to the difference in stability associated with the degree of electronic delocalization and number of the ferrocene moieties in the complexes. Crystal structure analysis indicates that the strong electronic donor of SCN^- as well as the intensive ferrocene moieties in single molecule in **1** may be major factors, result in the complex tending to be oxidized even more than the ligand. The chelating OAc^- can enhance the stability and degree of electronic delocalization of complex **2** with resulting increases in $E_{1/2}$ (ΔE_p).

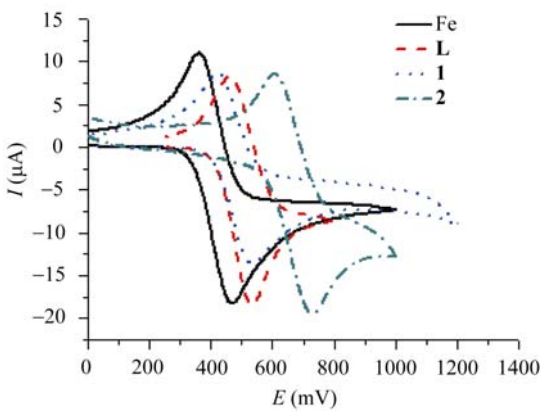

Figure 3 Cyclic-voltammetric response of 1 mmol·L^{-1} solution of **L**, **1** and **2** at the same scan rate of 50 mV/s in CH_2Cl_2 with 0.1 mol·L^{-1} TBAP at room temperature (vs. Ag/AgCl).

4 Supplementary materials

CCDC-276330 for **1** and CCDC-609285 for **2** contains

Table 4 CV data for **L**, **1** and **2**

Compounds	E_{pa} (V)	E_{pc} (V)	ΔE_p (V)	$E_{1/2}$ (V)[a)]	i_{pa} (μA)	i_{pc} (μA)	i_{pa}/i_{pc}
Ferrocene	0.470	0.362	0.108	0.416	17.99	16.73	1.075
L	0.536	0.461	0.075	0.500	18.13	16.60	1.052
1	0.533	0.422	0.111	0.478	13.24	12.20	1.110
2	0.726	0.608	0.118	0.667	19.43	17.66	1.100

a) vs. SCE.

the supplementary crystallographic data for this paper. These data can be obtained free of charge at http://www.ccdc.cam.ac.uk/conts/retrieving.html (or from the Cambridge Crystallographic Data Centre (CCDC), 12 Union Road, Cambridge CB2 1EZ, UK; fax: 44(0)1223-336033; e-mail: deposit@ccdc.cam.ac.uk).

1 Bard A J. Electron transfer branches out. Nature, 1995, 374: 13[DOI]
2 Mereacre V, Nakano M, Gomez-Segura J, Imaz I, Sporer C, Wurst K, Veciana J, Turta C, Ruiz-Molina D, Jaitner P. A new hexaferrocene complex with a $[M3(\mu3\text{-}O)]^{7+}$ core. Inorg Chem, 2006, 45(26): 10443－10445[DOI]
3 Saweczko P, Kraatz H B. The interaction of ferrocenoyl peptides with 3-aminopyrazole. Coord Chem Rev, 1999, 190: 185－198 [DOI]
4 Delavaux-Nicot B, Maynadie J, Lavabre D, Fery-Forgues S. Ferrocenyl compound as a multiresponsive calcium chemosensor with remarkable fluorescence properties in CH_3CN. Inorg Chem, 2006, 45(14): 5691－5702[DOI]
5 Welton T. Room-temperature ionic liquids. Solvents for synthesis and catalysis. Chem Rev, 1999, 99(8): 2071－2084[DOI]
6 Daniel M C, Ruiz J, Astruc D. Supramolecular H-bonded assemblies of redox-active metallodendrimers and positive and unusual dendritic effects on the recognition of $H_2PO_4^-$. J Am Chem Soc, 2003, 125(5): 1150－1151[DOI]
7 Gao Y, Twamley B, Shreeve J M. The first (ferrocenylmethyl)imidazolium and (ferrocenylmethyl)triazolium room temperature ionic liquids. Inorg Chem, 2004, 43(11): 3406－3412[DOI]
8 Mata J A, Peris E, Llusar R, Uriel S, Cifuentes M P, Humphrey M G, Samoc M, Luther-Davies B. Syntheses, structures and nonlinear optical properties of ferrocenyl complexes with arylethenyl substituents. Eur J Inorg Chem, 2001, 8: 2113[DOI]
9 Barlowa S, Marder S R. Electronic and optical properties of conjugated group 8 metallocene derivatives. Chem Commun, 2000, 17: 1555－1562[DOI]
10 Astruc D, Chardac F. Dendritic catalysts and dendrimers in catalysis. Chem Rev, 2001, 101(9): 2991－3024[DOI]
11 Horikoshi R, Mochida T, Moriyama H. Synthesis and characterization of redox-active coordination polymers generated from ferrocene-containing bridging ligands. Inorg Chem, 2002, 41(11): 3017－3024 [DOI]
12 Paris S I M, Petersen J L, Hey-Hawkins E, Jensen M P. Spectroscopic characterization of primary and secondary phosphine ligation on ruthenium(II) complexes. Inorg Chem, 2006, 45(14): 5561－5567[DOI]
13 Tarrasa A, Molina P, Curiel D, Velasco M D. Homotrimetallic oxazolo-ferrocene complexes displaying tunable cooperative interactions between metal centers and redox-switchable character. Organometallics, 2001, 20(11): 2145－2152[DOI]
14 Beer P D. Transition-metal receptor systems for the selective recognition and sensing of anionic guest species. Acc Chem Res, 1998, 31(2): 71－80[DOI]
15 Jautze S, Seiler P, Peters R. Macrocyclic ferrocenyl-bisimidazoline palladacycle dimers as highly active and enantioselective catalysts for the aza-claisen rearrangement of Z-configured N-para-methoxyphenyl trifluoroacetimidates. Angew Chem Int Ed, 2007, 46(8): 1260－1264[DOI]
16 Osakada K, Sakano T, Horie M, Suzaki Y. Functionalized ferrocenes: Unique properties based on electronic communication between amino group of the ligand and Fe center. Coord Chem Rev, 2006, 250(9): 1012－1022[DOI]
17 Zheng G L, Ma J F, Su Z M, Yan L K, Yang J, Li Y Y, Liu J F. A mixed-valence tin-oxygen cluster containing six peripheral ferrocene units. Angew Chem Int Ed, 2004, 43: 2409－2411[DOI]
18 Bildstein B, Malaun M, Kopacka H, Wurst K, Mitterbock M, Ongania K H, Opromolla G, Zanello P. *N*,*N*'-diferrocenyl-*N*-heterocyclic carbenes and their derivatives. Organometallics, 1999, 18(21): 4325－4336[DOI]
19 Baskar V, Roesky P W. Lanthanide hydroxide cubane clusters anchoring ferrocenes: Model compounds for fixation of organometallic fragments on a lanthanide oxide surface. Dalton Trans, 2006, 5: 676－679[DOI]
20 Wang X F, Lv Y, Su Z, Okamura T, Wu G, Sun W Y, Ueyama N Z. Anion and additive effects on the structure of mercury(II) halides complexes with tripodal ligand. Anorg Allg Chem, 2007, 633: 2695－2700[DOI]
21 Tian Y Q, Chen Z X, Weng L H, Guo H B, Gao S, Zhao D Y. Two polymorphs of cobalt(II) imidazolate polymers synthesized solvothermally by using one organic template *N*,*N*-dimethylacetamide. Inrog Chem, 2004, 43(15): 4631－4635[DOI]
22 Norberto M, Attilio GA, Stefano B, Fulvio C, Simona G, Angelo M, Angelo S. Synthesis and *ab-initio* XRPD structure of group 12 imidazolato polymers. Chem Commun, 2003, 16: 2018－2019
23 Norberto M, Fulvio C, Paul M F, Maya M T. Synthesis and characterization of two polymorphic crystalline phases and an amorphous powder of nickel(II) bisimidazolate. Inorg Chem, 2003, 42(19): 6147－6152[DOI]
24 Ma J F, Yang J, Zheng G L, Li L, Liu J F. Anthony K C. A porous supramolecular architecture from a copper(II) coordination polymer with a 3D four-connected 86 net. Inorg Chem, 2003, 42(23): 7531－7534[DOI]
25 Jin F, Zhou H P, Wang X C, Hu Z J, Wu J Y, Tian Y P, Jiang M H. Synthesis, structures and photoluminescence of thiocyanate bridged metal-organic polymers containing functional imidazole ligand. Polyhedron, 2007, 26: 1338－1346[DOI]
26 Jin F, Li J F, Zhou H P, Wu J Y, Yang J X, Tian Y P, Jiang M H. Synthesis, crystal structures, and optical properties of a novel imidazole derivative and its Zn(II) complex. J Mol Struct, 2007, 829: 202－207[DOI]
27 Fan J, Sui B, Okamura T, Tang W X, Sun W Y, Ueyama N. Synthesis, structures and properties of two-dimensional honeycomb and stepwise networks from self-assembly of tripodal ligand 1,3,5-tris(imidazol-1-ylmethyl)-2,4,6-trimethylbenzene with metal salts. J Chem Soc Dalton Trans, 2002, 21: 3868－3873[DOI]
28 Sun W Y, Fan J, Okamura T, Ueyama N. Synthesis and structural characterization of a new one-dimensional chain coordination polymer of copper(II) with diethylenetriamine and 1,3-bis(imidazol-1-

ylmethyl)-5-methylbenzene. Inorg Chem Commun, 2000, 3(10): 541－544[DOI]
29 Snegur L V, Simenel A A, Nekrasov Y S, Morozova E A, Starikova Z A, Peregudova S M, Kuzmenko Y V, Babin V N, Ostrovskaya L A, Bluchterova N V, Fomina M M. Synthesis, structure and redox potentials of biologically active ferrocenylalkyl azoles. J Organometallic Chem, 2004, 689(15): 2473－2479[DOI]
30 Wang X C, Li J F, Wu J Y, Zhou H P, Yang J X, Jin B K, Tian Y P. Synthesis, crystal structure, electrochemical properties and large optical limiting effect of a novel 3-(*E*)-ferrocenyl-vinyl-*N*-hexyl carbazole. Trans Metal Chem, 2007, 32: 551－557[DOI]
31 Yang J X, Tao X T, Yuan C X, Yan Y X, Wang L, Liu Z, Ren Y, Jiang M H. A facile synthesis and properties of multicarbazole molecules containing multiple vinylene bridges. J Am Chem Soc, 2005, 127(10): 3278－3279[DOI]
32 Sheldrick G M. SHELXS97 and SHELXL-97. Göttingen: University of Göttingen, 1997
33 Gao Y, Twamley B, Shreeve J M. Supramolecular networks using ferrocenyl ditriazole and diimidazole bridges. Organometallics, 2006, 25(14): 3364－3369[DOI]
34 Horikoshi R, Nambu C, Mochida T. Metal-centered ferrocene clusters from 5-ferrocenylpyrimidine and ferrocenylpyrazine. Inorg Chem, 2003, 42(21): 6868－6875[DOI]
35 Barszcz B. Coordination properties of didentate N, O heterocyclic alcohols and aldehydes towards Cu(II), Co(II), Zn(II) and Cd(II) ions in the solid state and aqueous solution. Coord Chem Rev, 2005, 249: 2259－2276[DOI]
36 Kuhn N, Al-Sheikh A. 2, 3-Dihydroimidazol-2-ylidenes and their main group element chemistry. Coord Chem Rev, 2005, 249(7): 829－857[DOI]
37 Zhou H P, Wang P, Hu Z J, Li L, Cui Y, Tian Y P, Wu J Y, Yang J X, Tao X T, Jiang M H. Synthesis, crystal structures, and photoluminescence of a series of coordination polymers with two homologous functional flexible ligands. Eur J Inorg Chem, 2007, 13: 1854－1866[DOI]
38 Bond A D, Jones W. Divalent complexes of 3-hydroxy-4-methyl-2(3H)-thiazolethione with Co-Zn: Synthesis, X-ray crystal structures and the structure-directing influence of C-HS interactions. J Chem Soc Dalton Trans, 2001, 20: 3045－3051[DOI]
39 Zhou H P, Zhu Y M, Chen J J, Hu Z J, Wu J Y, Xie Y, Tao X T, Jiang M H, Tian Y P. A new ligand for the formation of a 3D structure by significant C–H···S hydrogen bonds and π–π interactions. Inorg Chem Commun, 2006, 9(1): 90－92[DOI]
40 Braga D, Polito M, D'Addario D, Tagliavini E, Proserpio D M, Grepioni F, Steed J W. Design, synthesis, and structural characterization of molecular and supramolecular heterobimetallic metallamacrocycles based on the 1,1'-bis(4-pyridyl)ferrocene (Fe(η^5-C_5H_4-1-$C_5H_4N)_2$) ligand. Organometallics, 2003, 22(22): 4532－4538[DOI]
41 Horikoshi R, Nambu C, Mochida T. Metal-centered ferrocene clusters from 5-ferrocenylpyrimidine and ferrocenylpyrazine. Inorg Chem, 2003, 42(21): 6868－6875[DOI]
42 Kuhn N, Al-Sheikh A. 2, 3-Dihydroimidazol-2-ylidenes and their main group element chemistry. Coord Chem Rev, 2005, 249: 829－857[DOI]
43 Duan C Y, Tian Y P, Liu Z H, You X Z, Thomas C W. Syntheses, electrochemistry and crystal structure studies of novel *cis*-configuration biferrocene trinuclear complexes. J Organometallic Chem, 1998, 570(2): 155－162[DOI]